REVIEW

Bioactive metals: preparation and properties

T. KOKUBO
Research Institute of Science and Technology, Chubu University, 1200 Matsumoto-cho, Kasugai-shi, Aichi 487-8501, Japan

H.-M. KIM*
Department of Ceramic Enginering, School of Advanced Materials Engineering, Yonsei University, 134 Shinchon-dong, Seodaemun-gu, Seoul 120-749, Korea
E-mail: hmkim@yonsei.ac.kr

M. KAWASHITA
Department of Material Chemistry, Graduate School of Engineering, Kyoto University, Yoshida, Sakyo-ku, Kyoto 606-8501, Japan

T. NAKAMURA
Department of Orthopaedic Surgery, Graduate School of Medicine, Kyoto University, Kawahara, Sakyo-ku, Kyoto 606-8507, Japan

Some ceramics, such as Bioglass®, sintered hydroxyapatite, and glass-ceramic A-W, spontaneously form a bone-like apatite layer on their surface in the living body, and bond to bone through the apatite layer. These materials are called bioactive ceramics, and are clinically important for use as bone-repairing materials. However, they cannot be used at high-load sites, such as is found in femoral and tibial bones, because their fracture toughness values are not as high as that of human cortical bone. Titanium metal and its alloys have high fracture toughness, and form a sodium titanate layer on its surface when soaked in a 5 M-NaOH solution at 60 °C for 24 h, followed by a heat treatment at 600 °C for 1 h. On moving toward the metal interior, the sodium titanate layer gradually changes into the pure metal within a distance of 1 μm from the surface. The mechanical strength of the titanium metal or a titanium alloy is not adversely affected by these chemical and thermal treatments. The titanium metal and its alloys resulting from the above treatment can release Na^+ ions from its surface into a surrounding body fluid via an ion exchange reaction with H_3O^+ ions, resulting in many Ti–OH groups forming on its surface. These Ti–OH groups initially combine with Ca^{2+} ions to form amorphous calcium titanate in the body environment, and later the calcium titanate combines with phosphate ions to form amorphous calcium phosphate. The amorphous calcium phosphate eventually transforms into bone-like apatite, and by this process the titanium metals are soon tightly bonded to the surrounding living bone through the bone-like apatite layer. The treated metals have already been subjected to clinical trials for applications in artificial total hip joints. Metallic tantalum has also been found to bond to living bone after it has been subjected to the NaOH and heat treatment to form a sodium tantalate layer on its surface.

1. Introduction

Artificial materials implanted into bone defects are generally encapsulated by a fibrous tissue so that they are isolated from the surrounding bone. However, some ceramics, such as Bioglass® [1], sintered hydroxyapatite [2], and glass-ceramic A-W [3], spontaneously bond to living bone without forming a surrounding fibrous tissue. These ceramics are called bioactive ceramics, and have an important clinical function as bone-repairing materials [2, 4–6]. However, even glass-ceramic A-W, which has the highest mechanical strength among the above materials, cannot be used in load-bearing applications, such as those encountered in femoral and tibial bones. In these applications, metallic materials, such as stainless steel, Co–Cr–Mo alloys, and titanium alloys are used. However, these materials do not directly

*Author to whom all correspondence should be addressed.

bond to living bone. Therefore, they are often used after being coated with hydroxyapatite using the plasma spraying method [7]. In this technique, hydroxyapatite powder is briefly melted in a flame at temperatures $> 10\,000\,^{\circ}C$ and the hydroxyapatite is partially decomposed. The resultant coating is not stable for long periods in the living body. Therefore, it is most desirable for the metallic materials themselves to exhibit a bone-bonding ability, i.e. bioactivity.

Recently, we revealed that titanium and tantalum metals and their alloys spontaneously bond to living bone if they have been previously subjected to a treatment involving a soak in NaOH solution followed by a subsequent heat treatment. These metals can therefore be called bioactive metals, and are already subjected to clinical trials for use in artificial total hip joints. This article describes the preparation and properties of these bioactive metals.

2. Fundamentals of bioactivity

2.1. The prerequisite for bioactivity

All the bioactive ceramics described above form an apatite layer on their surface in the living body, and bond to living bone through this apatite layer [8]. The formed apatite is very similar to bone mineral in its composition and structure [9]. Therefore, osteoblasts preferentially proliferate and differentiate to produce apatite and collagen on this apatite layer [10], and, consequently, the surrounding bone can come into direct contact with the surface apatite layer. When this occurs, a strong chemical bond is formed between the bone minerals and the surface apatite layer to reduce the interface energy between them [11]. This indicates that the essential requirement for an artificial material to bond to living bone is the formation of a biologically active bone-like apatite layer on its surface in the living body [12].

2.2. The prerequisite for apatite formation

Human body fluid is supersaturated with respect to apatite even under normal conditions [13, 14]. The fact that apatite formation only occurs in bone tissue in the human body is attributed to the high activation energy for the homogeneous nucleation of apatite in human body fluid. Therefore, if an artificial material has a functional group that could be an effective apatite nucleation site on its surface, then it will easily form apatite nuclei on its surface. Once the apatite nuclei are formed, they would spontaneously grow by consuming calcium and phosphate ions from the surrounding body fluid. The prerequisite for apatite formation on an artificial material in a living body is the presence of a type of functional groups that could be an effective site for apatite nucleation on its surface [15].

2.3. Functional groups effective for apatite nucleation

When various metal oxide gels are prepared using the sol–gel method and soaked in a simulated body fluid (SBF) with ion concentrations (Na^+ 142.0, K^+ 5.0, Ca^{2+} 2.5, Mg^{2+} 1.5, Cl^- 147.8, HCO^{3-} 4.2, HPO_4^{2-} 1.0, SO_4^{2-} 0.5 mM, pH 7.40) nearly equal to those of human blood plasma, SiO_2 [16], TiO_2 [17], ZrO_2 [18], Nb_2O_5 [19], and Ta_2O_5 [20] gels form bone-like apatite on their surfaces, as shown in Fig. 1, but Al_2O_3 gel does not [17]. This indicates that the abundant Si–OH, Ti–OH, Zr–OH, Nb–OH, and Ta–OH groups on the gels are effective for apatite nucleation, and that the Al–OH group is not effective for apatite nucleation. All the former gels are negatively charged in an SBF at pH = 7.4, but an Al_2O_3 gel is positively charged.

3. Preparation of bioactive metal

3.1. The formation of Ti–OH groups on titanium metal

Titanium metal is generally covered with a thin TiO_2 passive layer, and hence is chemically durable. However,

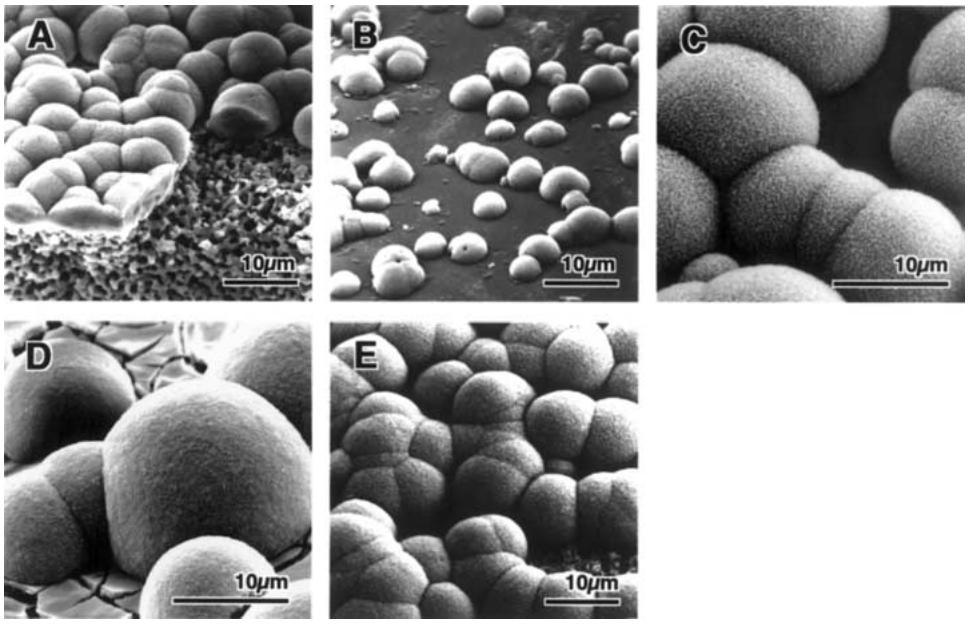

Figure 1 Bone-like apatite formation induced on SiO_2 (A), TiO_2 (B), ZrO_2 (C), Ta_2O_5 (D), and Nb_2O_5 (E) gels in SBF.

even this stable TiO_2 layer reacts with NaOH solution to form a sodium titanate gel, and this gel layer can be stabilized as an amorphous sodium titanate layer by a suitable heat treatment. Such a sodium titanate layer is expected to form many Ti–OH groups on its surface in the living body via the ion exchange of its Na^+ ions from the surface with H_3O^+ ions in the surrounding body fluid.

Fig. 2 shows depth profiles of the Auger electron spectra of Ti, Na, and O from titanium metal samples taken before and after soaking in a 5 M-NaOH solution at 60 °C for 24 h, followed by heat treatment at 600 °C for 1 h [21–25]. Fig. 2 confirms that a sodium titanate layer with a graded structure is formed, in which the sodium titanate gradually changes to titanium metal on moving towards the interior, and that this transition occurs within a depth of 1 μm from the surface of the titanium metal after the NaOH treatment. This graded structure is essentially unchanged by the subsequent heat treatment, although some oxygen penetrates into a little deeper region.

According to thin-film X-ray diffraction and Raman spectroscopy, the sodium titanate layer after the NaOH treatment has a gel-like structure [21–23], and has an essentially an amorphous structure after the subsequent heat treatment [24]. The gel layer of sodium titanate can be scratched with a diamond needle under a load as low as 5 grf, whereas a load as high as 30 grf is needed to scratch the amorphous layer of sodium titanate [24].

Fig. 3 shows the X-ray photoelectron spectra of the Na and O from the NaOH- and heat-treated titanium metal as a function of soaking time in the SBF [24, 27]. From Fig. 3 it can be seen that the Na^+ ions are rapidly released from the surface into the SBF, and that Ti–OH groups are formed on the surface as the Na^+ ions are released, as was expected.

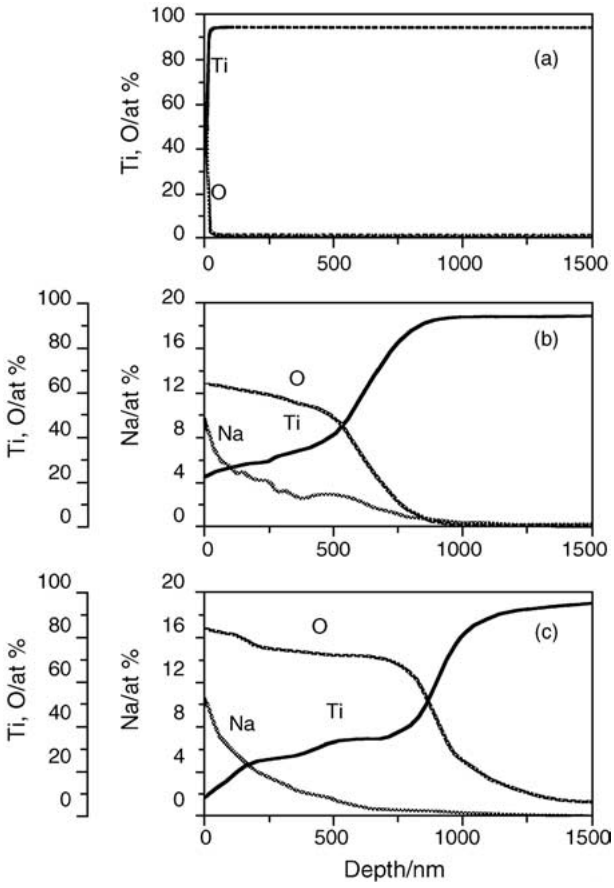

Figure 2 Depth profiles of Auger electron spectra of Ti, Na, and O of a titanium metal before (A) and after soaking in 5 M-NaOH solution at 60 °C for 24 h (B), and after subsequent heat treatment at 600 °C for 1 h (C).

3.2. The effect of the NaOH and heat treatments on the mechanical properties of titanium metal

For a bone-repairing material for use under load-bearing conditions, any Ti–OH groups must form on its surface without causing any detrimental effect on the mechanical properties.

Fig. 4 shows the number of the loading cycles to failure for the NaOH- and heat-treated titanium metals, when various loads were applied at a frequency of 5 Hz in a saline solution at 37 °C, and these are compared with the results obtained on untreated titanium metal [28]. It

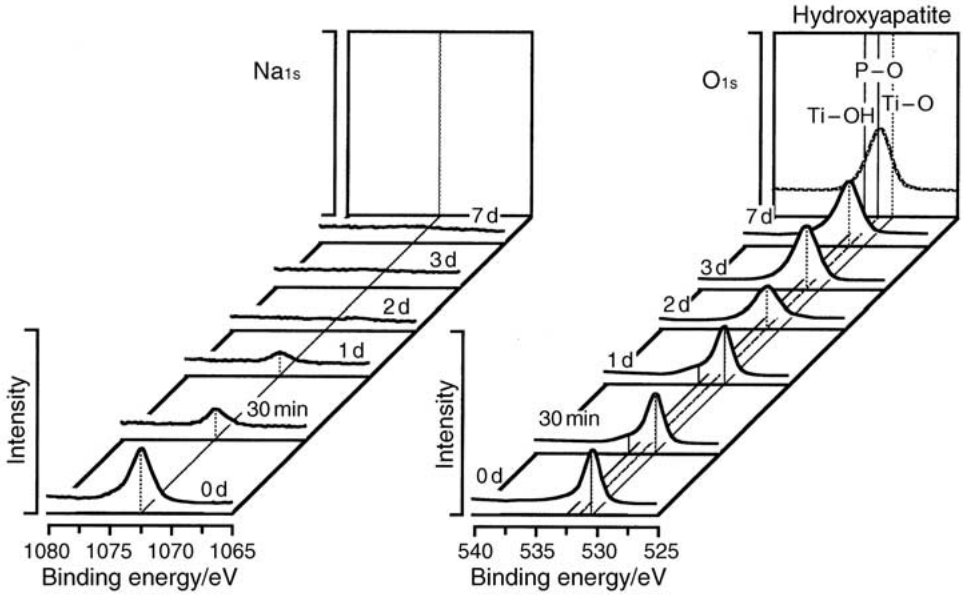

Figure 3 X-ray photoelectron spectra of Na and O of the NaOH- and heat-treated titanium metal as a function of soaking time in SBF.

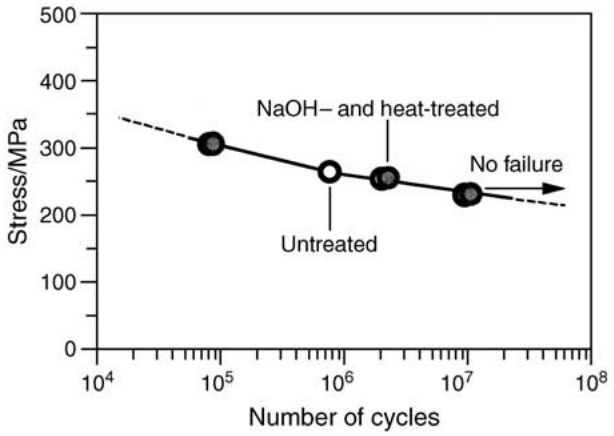

Figure 4 Number of the cycles of loading to the failure of the untreated and the NaOH- and heat-treated titanium metals.

can be confirmed from the results shown in Fig. 4 that the NaOH and heat treatments do not have any adverse effect on the mechanical fatigue properties of the titanium metal.

3.3. Apatite formation on NaOH- and heat-treated titanium metal and its alloys

To examine the possibility of *in vivo* apatite formation on the NaOH- and heat-treated titanium metal, a titanium metal grid which had been subjected to the NaOH and heat treatments was soaked in an SBF at 36.5 °C for various periods, and examined using transmission electron microscopy (TEM) and energy-dispersive X-ray analysis (EDX) [29].

Fig. 5 shows a TEM–EDX observation of an edge of the NaOH- and heat-treated titanium grid before and after soaking in an SBF for various periods. Fig. 5 confirms that the surface of the titanium metal subjected to the NaOH and heat treatments is covered with a porous amorphous sodium titanate layer containing a small quantity of crystalline sodium titanate ($Na_2Ti_5O_{11}$) and rutile (TiO_2). After soaking in an SBF for 30 min, the sodium peak decreased, and a new calcium peak was observed in the EDX spectrum. No new distinct line was observed on the electron diffraction pattern. This means that Ti–OH groups, which were formed by the exchange of Na^+ ions with H_3O^+ ions, initially combine with the calcium ions in the SBF to from amorphous calcium titanate. After soaking in the SBF for 1.5 days, strong Ca and P peaks were observed in the EDX spectra, while the electron diffraction data showed no distinct pattern. This means that amorphous calcium phosphate was newly formed. The observed Ca/P atomic ratio was 1.40, which is much lower than that of bone apatite, with a Ca/P atomic ratio of 1.65. After soaking in the SBF for 5 days, nano-sized needle-like particles were observed, which gave a distinct electron diffraction pattern that could be ascribed to apatite. These particles had a Ca/P ratio of 1.65, and showed small Na and Mg peaks in the EDX spectra, similar to those seen for bone apatite. This means that bone-like apatite had formed on the metal.

To examine why apatite was formed by this process, the variation of the zeta potential of the NaOH- and heat-treated titanium metal during soaking in the SBF was measured using laser electrophoresis analysis [30]. The zeta potential of the treated titanium metal initially gave a negative value in the SBF, but increased with increasing soaking time, passing through a maximum positive value, and then decreasing to a negative value, as shown in Fig. 6. Based on this result, the process of apatite

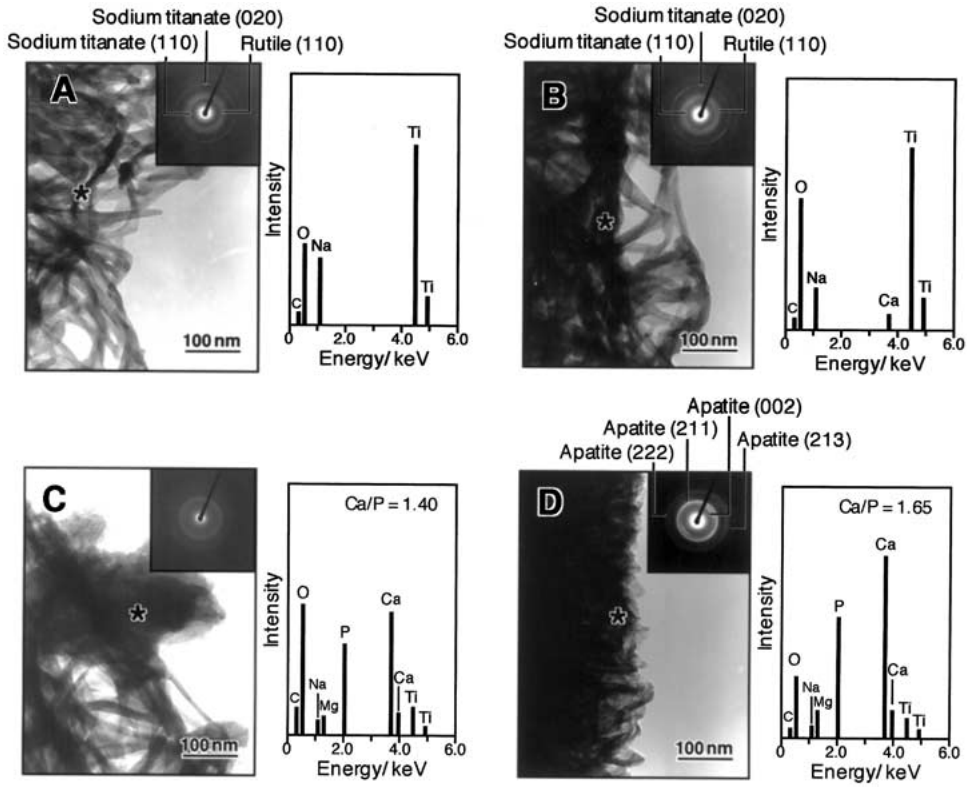

Figure 5 TEM–EDX profiles of the surface of the NaOH- and heat-treated titanium metal before (A) and after soaking in SBF for 30 min (B), 1.5 days (C) and 5 days (D) (*: Center of the electron diffraction and EDX analyses).

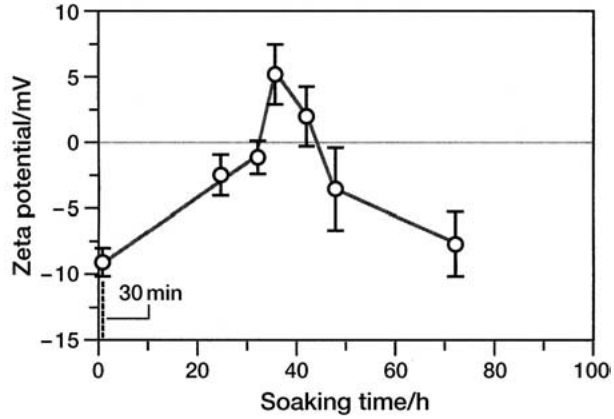

Figure 6 Variation of zeta potential of the NaOH- and heat-treated titanium metal with soaking time in SBF.

formation on the treated titanium metal is interpreted in terms of an electrostatic interaction, as shown in Fig. 7.

The Ti–OH groups formed by the exchange of Na^+ and H_3O^+ ions are negatively charged in the SBF at pH = 7.4, and hence they initially combine with the positively charged Ca^{2+} ions in the SBF to form amorphous calcium titanate. As the Ca^{2+} ions accumulate, the calcium titanate becomes positively charged, and hence it then combines with the negatively charged phosphate ions in the SBF to form amorphous calcium phosphate. Because amorphous calcium phosphate is metastable in an SBF, it eventually transforms into crystalline apatite. Once apatite nuclei are formed, they spontaneously grow by consuming the calcium and phosphate ions from the SBF to form a dense and uniform apatite layer, as shown in Fig. 8 [21, 22].

The same type of apatite layer is formed not only on pure titanium metal, but also on titanium-based alloys in an SBF, such as Ti–6Al–4V [31, 32], Ti–6Al–2Nb–Ta [22] and Ti–15Mo–5Zr–3Al [33] provided that they have been subjected to the NaOH and heat treatments. The alloying metals, such as Al and V, are selectively released during the NaOH treatment [31, 33].

3.4. Bonding of the apatite layer to titanium metal

Fig. 9 shows the depth profile of the Auger electron spectra of Na, Ca, P, O, and Ti of the treated titanium metal that had formed an apatite layer in the SBF [25]. From Fig. 9 it can be seen that the apatite gradually changes into titanium metal on moving towards the interior. This means that the apatite layer is tightly integrated into the titanium substrate. Because of the existence of this graded structure, the apatite layer cannot delaminate from the substrate; however, fractures can occur at the interface between the apatite and a jig when under a tensile load [33].

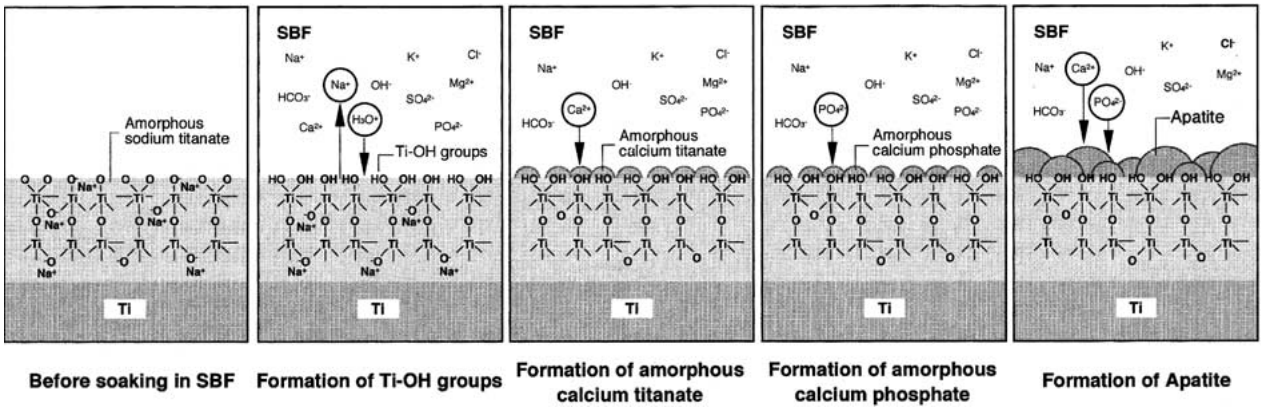

Figure 7 Mechanism of the apatite formation on the NaOH- and heat-treated titanium metal in SBF.

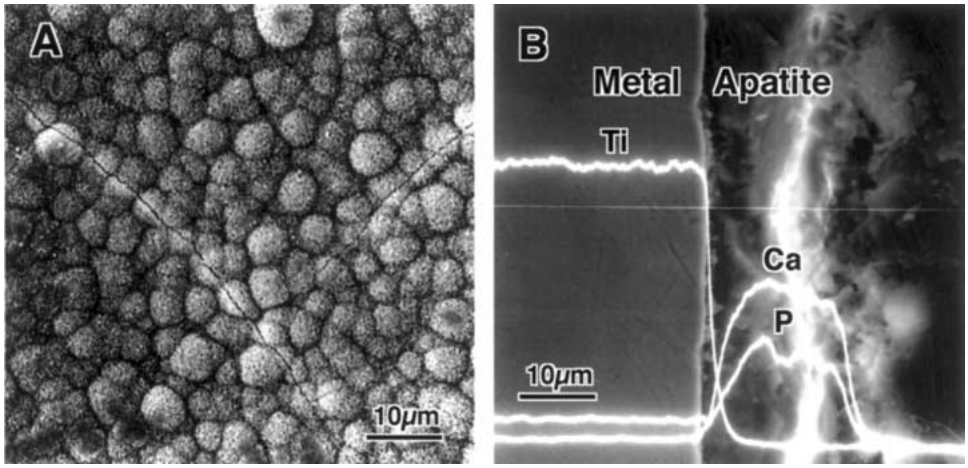

Figure 8 SEM–EDX profiles of the surface (A) and cross-section (B) of the NaOH- and heat-treated titanium metal after soaking in SBF for 28 days.

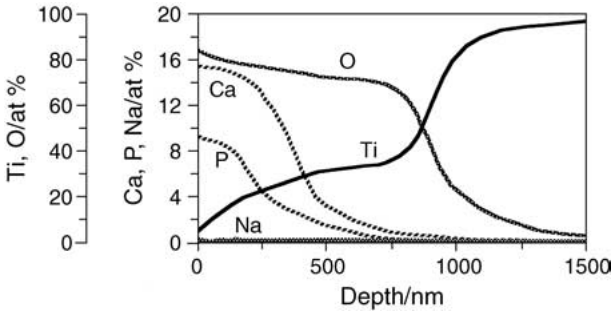

Figure 9 Depth profile of Auger electron spectra of Na, Ca, P, O, and Ti of the NaOH- and heat-treated titanium metal after soaking in SBF for 3 days.

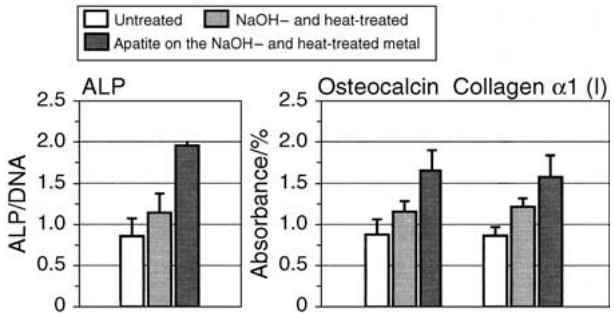

Figure 10 Production of alkaline phosphotase (ALP), osteocalcin, and type-I collagen on the untreated, the NaOH- and heat-treated titanium metals, and the apatite formed on the NaOH- and heat-treated titanium metal in SBF after rat bone marrow cell culture for 14 days.

4. Properties of bioactive metal

4.1. Osteoblast activity on the NaOH- and heat-treated titanium metal

The same type of bone-like apatite layer as that formed in the SBF is expected to form on the NaOH- and heat-treated titanium metal in a living body, and osteoblasts are expected to be activated on the bone-like apatite layer. To examine whether this could occur *in vitro*, rat bone marrow cells were cultured on untreated titanium metal, NaOH- and heat-treated titanium metal and also on the apatite formed on the NaOH- and heat-treated titanium metal [35]. Fig. 10 shows the production of alkaline phosphatase, osteocalcin, and type-I collagen on their surfaces after cultured for 14 days. It can be seen from Fig. 10 that the production of the above substances

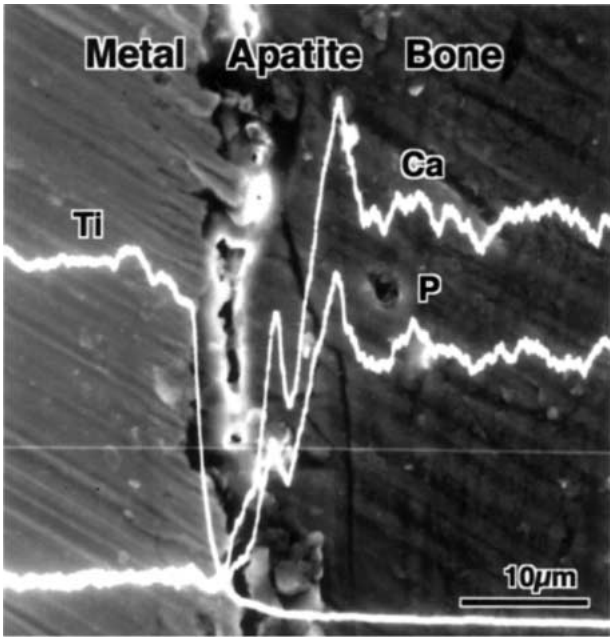

Figure 11 SEM–EDX profile of the interface between the NaOH- and heat-treated titanium metal and the rabbit tibia after implantation for 8 weeks.

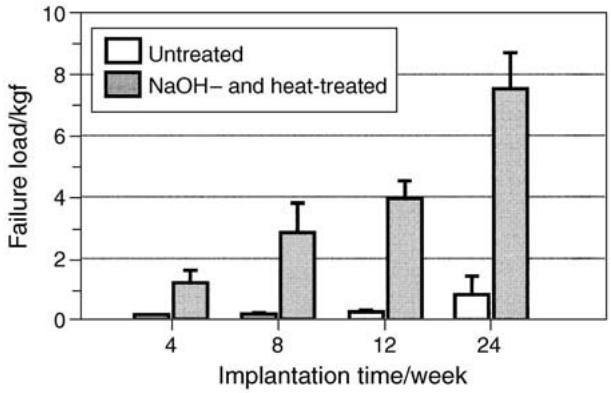

Figure 12 Detaching failure loads of the untreated and the NaOH- and heat-treated titanium metals implanted into rabbit tibia for various periods.

was more pronounced with the NaOH- and heat-treated titanium metal along with the formation of apatite than for the untreated titanium metal.

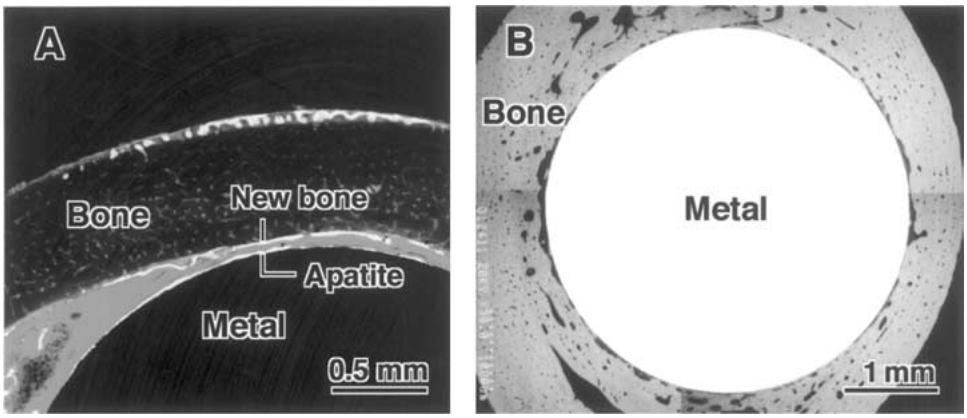

Figure 13 Confocal laser scanning micrograph (A) and SEM photograph (B) of a cross-section of the NaOH- and heat-treated titanium rod 3 and 112 weeks after implantation, respectively.

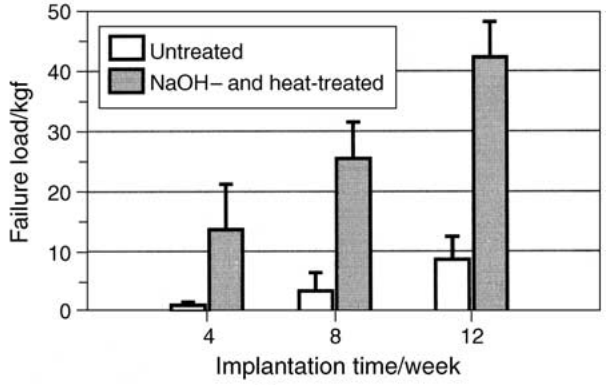

Figure 14 Pull-out failure loads of the untreated and the NaOH- and heat-treated titanium metal rods implanted into intramedullar canal of rabbit femur for various periods.

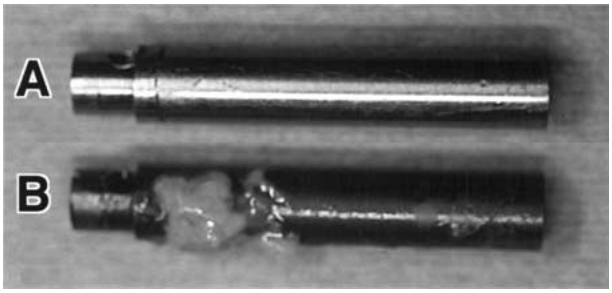

Figure 15 The untreated (A) and the NaOH- and heat-treated (B) titanium metal rods retrieved after implantation into intramedullar canal of rabbit femur for 12 weeks.

4.2. Bonding of bone with the NaOH- and heat-treated titanium metal

A $10 \times 15 \times 2\,mm^3$ rectangular specimen of the NaOH- and heat-treated titanium metal was implanted into the tibia of rabbit. The treated metal formed a bone-like apatite layer on its surface after implantation in the tibia, and bonded to the surrounding bone through this apatite layer, as shown in Fig. 11 [36–40]. When a tensile stress test was carried out on the sample, a much higher load was required to produce failure at the interface for the treated titanium metal than for samples of untreated titanium metal. The difference between the treated and untreated titanium increased remarkably with increasing implantation period, as shown in Fig. 12.

A rod of the NaOH- and heat-treated titanium metal (diameter = 5 mm, length = 25 mm) was implanted into the intramedullar canal of a femur of rabbit to model the stem of a hip joint [41, 42]. Fig. 13 shows a confocal laser scanning micrograph and SEM photograph of a cross-section of the rod after 3 and 12 weeks implantation, respectively. It can be seen from Fig. 13 that the rod had formed an apatite layer on its surface within 3 weeks, and was completely surrounded with newly formed bone within 12 weeks. When the rod was extracted from the surrounding bone, a much higher load was required for the treated titanium metal than for the untreated titanium metal. The difference between the treated and untreated titanium metals increased remarkably with increasing implantation period, as shown in Fig. 14. Twelve weeks after implantation, the treated metal could only be extracted with accompanying bone fragments, as shown in Fig. 15.

The above results are for titanium metal having a smooth surface. When titanium metal is formed having a macroporous structure, and then subjected to the NaOH and heat treatments, it forms a bone-like apatite layer along the surface of the pore walls [43, 44] and is penetrated with newly formed bone into even the most deeply seated pores [44]. In this case, the metal can bond to living bone by the chemical bonding mechanism described above; in addition, it can bond to living bone by a mechanical interlocking mechanism.

5. Perspectives of bioactive metal

5.1. The clinical application of bioactive metals

Bioactive titanium metal and its alloys are expected to be useful as bone substitutes in load-bearing conditions, such as those seen in total hip and knee replacement joints, dental implants, and in spinal cages. Clinical trials of their application in artificial total hip joints began in September 2000. In these trials, a titanium macroporous

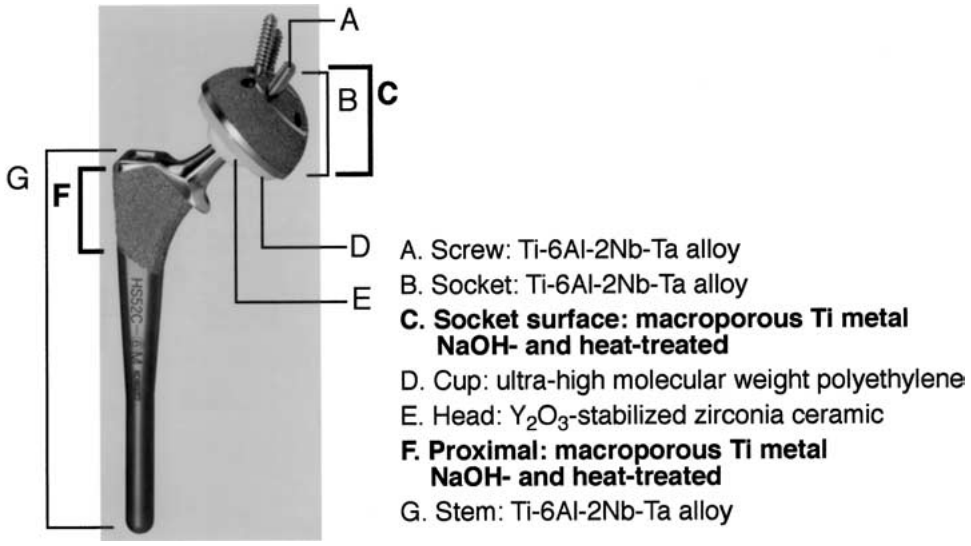

Figure 16 Application of the NaOH and heat treatments to titanium alloys in clinical hip joint system (photograph courtesy of Kobe Steel Ltd., Japan).

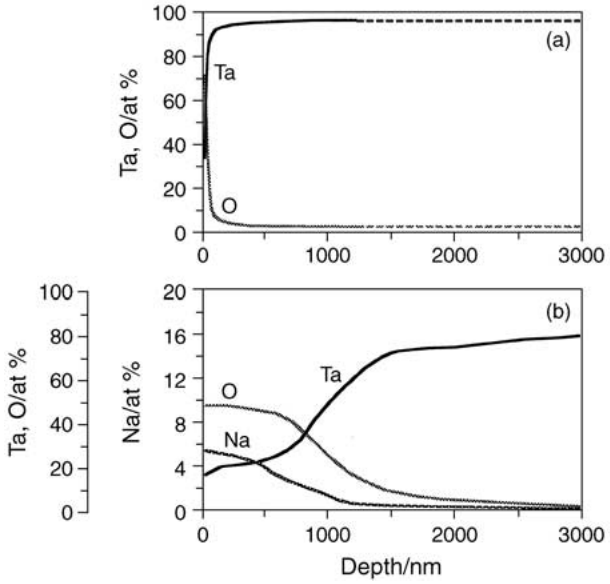

Figure 17 Depth profiles of Auger electron spectra of Ta, O, and Na of tantalum metal before (A) and after 0.5 M-NaOH treatment at 60 °C for 24 h and subsequent heat treatment at 300 °C for 1 h (B).

structure was formed on the surface of a titanium alloy for a proximal site stem, and on the whole surface of a titanium alloy cover of a polyethylene cup, and then these were subjected to the NaOH and heat treatments, as shown in Fig. 16. More than 70 patients have received this type of hip joint, and it has been reported to function very well.

5.2. Preparation of bioactive tantalum metal

The Ta–OH groups are also effective for apatite nucleation, when using the same preparative method as described above. The Ta–OH groups form on tantalum metal when it is subjected to a similar NaOH and heat treatment, and then implanted into a living body.

Fig. 17 shows the depth profiles of the Auger electron spectra of Ta, O, and Na of a tantalum metal sample, before and after a 0.5 M-NaOH treatment at 60 °C for 24 h, followed by a subsequent heat treatment at 300 °C for 1 h [45, 46]. It can be seen from Fig. 17 that a sodium tantalate layer with a graded structure is formed within a depth of 1 μm from the surface, and that its graded structure is not essentially changed by the heat treatment. According to thin-film X-ray diffraction and Raman spectra, the former layer assumes a gel structure, and the latter layer assumes an amorphous structure [47].

X-ray photoelectron spectroscopy confirms that the amorphous sodium tantalate layer produced forms Ta–OH groups on its surface in an SBF via an ion exchange of its Na^+ ions with H_3O^+ ions in the SBF, and that the Ta–OH groups formed induce apatite nucleation by initially combining the Ca^{2+} ions, and later these combine with the phosphate ions in the SBF [47].

When the treated tantalum metal is implanted into the tibia of a rabbit, it forms an apatite layer on its surface, and bonds to the living bone through the apatite layer, as shown in Fig. 18 [48].

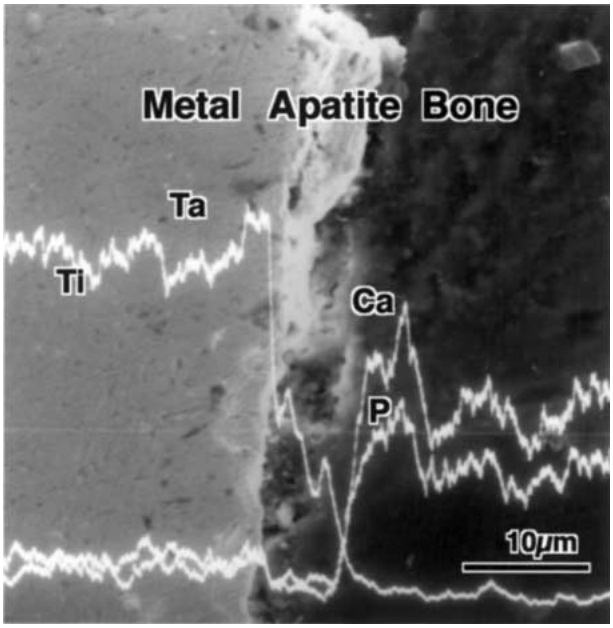

Figure 18 SEM–EDX profile of the interface between the NaOH- and heat-treated tantalum metal and the rabbit tibia after implantation for 8 weeks.

6. Summary

Bioactive metals can be prepared by simple chemical and moderate heat treatments. This class of bioactive material has high fracture toughness, and could find a wide use as bone-repairing materials in load-bearing applications.

References

1. L. L. HENCH and Ö. H. ANDERSSON, in ''An Introduction to Bioceramics'' (World Scientific, Singapore, 1993) p. 41.
2. R. Z. LEGEROS and J. P. LEGEROS, in ''An Introduction to Bioceramics'' (World Scientific, Singapore, 1993) p. 139.
3. T. KOKUBO, in ''An Introduction to Bioceramics'' (World Scientific, Singapore, 1993) p. 75.
4. J. WILSON, A. YLI-URPO and H. RISTO-PEKKA, in ''An Introduction to Bioceramics'' (World Scientific, Singapore, 1993) p. 63.
5. E. C. SHORES and R. E. HOLMES, in ''An Introduction to Bioceramics'' (World Scientific, Singapore, 1993) p. 181.
6. T. YAMAMURO, in ''An Introduction to Bioceramics'' (World Scientific, Singapore, 1993) p. 89.
7. W. R. LACEFIELD, in ''An Introduction to Bioceramics'' (World Scientific, Singapore, 1993) p. 223.
8. N. NEO, S. KOTANI, T. NAKAMURA, T. YAMAMURO, C. OHTSUKI, T. KOKUBO and Y. BANDO, *J. Biomed. Mater. Res.* **26** (1992) 1419.
9. T. KOKUBO, S. ITO, Z. T. HUANG, T. HAYASHI, S. SAKKA, T. KITSUGI and T. YAMAMURO, *ibid.* **24** (1990) 331.
10. M. NEO, T. NAKAMURA, C. OHTSUKI, T. KOKUBO and T. YAMAMURO, *ibid.* **27** (1993) 999.
11. T. KOKUBO, T. HAYASHI, S. SAKKA, T. KITSUGI and T. YAMAMURO, *J. Ceram. Soc. Japan* (Yogyo-Kyokai-Shi) **95** (1987) 785.
12. T. KOKUBO, *Biomaterials* **12** (1991) 155.
13. W. NEUMAN and M. NEUMAN, in ''The Chemical Dynamics of Bone Mineral'' (University of Chicago Press, IL, 1958) p. 1.
14. J. GAMBLE, in ''Chemical Anatomy, Physiological and Pathology of Extracellular Fluid'' (Harvard University Press, MA, 1967) p. 1.
15. C. OHTSUKI, T. KOKUBO and T. YAMAMURO, *J. Non-Cryst. Solids* **143** (1992) 84.
16. P. LI, C. OHTSUKI, T. KOKUBO, K. NAKANISHI, N. SOGA, T. NAKAMURA and T. YAMAMURO, *J. Am. Ceram. Soc.* **75** (1992) 2094.

17. P. LI, C. OHTSUKI, T. KOKUBO, K. NAKANISHI, N. SOGA, T. NAKAMURA, T. YAMAMURO and K. DE GROOT, *J. Biomed. Mater. Res.* **28** (1994) 7.
18. M. UCHIDA, H.-M. KIM, T. KOKUBO and T. NAKAMURA, *J. Am. Ceram. Soc.* **84** (2001) 2041.
19. T. MIYAZAKI, H.-M. KIM, T. KOKUBO, C. OHTSUKI, H. KATO and T. NAKAMURA, *J. Ceram. Soc. Japan* **109** (2001) 929.
20. T. MIYAZAKI, H.-M. KIM, T. KOKUBO, H. KATO and T. NAKAMURA, *J. Sol-Gel Sci. Tech.* **21** (2001) 83.
21. T. KOKUBO, F. MIYAJI, H.-M. KIM and T. NAKAMURA, *J. Am. Ceram. Soc.* **79** (1996) 1127.
22. H.-M. KIM, F. MIYAJI, T. KOKUBO and T. NAKAMURA, *J. Biomed. Mater. Res.* **32** (1996) 409.
23. H.-M. KIM, F. MIYAJI, T. KOKUBO and T. NAKAMURA, *J. Ceram. Soc. Japan* **105** (1997) 111.
24. H.-M. KIM, F. MIYAJI, T. KOKUBO and T. NAKAMURA, *J. Mater. Sci.: Mater. Med.* **8** (1997) 341.
25. H.-M. KIM, F. MIYAJI, T. KOKUBO, S. NISHIGUCHI and T. NAKAMURA, *J. Biomed. Mater. Res.* **45** (1999) 100.
26. H.-M. KIM, H. TAKADAMA, F. MIYAJI, T. KOKUBO and T. NAKAMURA, *Kor. J. Ceram.* **4** (1998) 336.
27. H. TAKADAMA, H.-M. KIM, T. KOKUBO and T. NAKAMURA, *J. Biomed. Mater. Res.* **55** (2001) 185.
28. H.-M. KIM, Y. SASAKI, J. SUZUKI, S. FUJIBAYASHI, T. KOKUBO, T. MATSUSHITA and T. NAKAMURA, in ''Bioceramics'', vol. 13 (Trans Tech Pub., Switzerland, 2000) p. 227.
29. H. TAKADAMA, H.-M. KIM, T. KOKUBO and T. NAKAMURA, *J. Biomed. Mater. Res.* **57** (2001) 441.
30. T. HIMENO, M. KAWASHITA, H.-M. KIM, T. KOKUBO and T. NAKAMURA, in ''Bioceramics'', vol. 14 (Trans Tech Pub., Switzerland, 2001) p. 641.
31. H.-M. KIM, H. TAKADAMA, F. MIYAJI, T. KOKUBO, S. NISHIGUCHI and T. NAKAMURA, *J. Mater. Sci.: Mater. Med.* **11** (2000) 555.
32. H. TAKADAMA, H.-M. KIM, T. KOKUBO and T. NAKAMURA, *Sci. Tech. Adv. Mater.* **2** (2001) 389.
33. H.-M. KIM, H. TAKADAMA, F. MIYAJI, T. KOKUBO, S. NISHIGUCHI and T. NAKAMURA, *Biomaterials* **21** (2000) 353.
34. H.-M. KIM, F. MIYAJI, T. KOKUBO and T. NAKAMURA, *J. Biomed. Mater. Res.* **38** (1997) 121.
35. K. NISHIO, M. NEO, H. AKIYAMA, S. NISHIGUCHI, H.-M. KIM, T. KOKUBO and T. NAKAMURA, *ibid.* **52** (2000) 652.
36. W. Q. YAN, T. NAKAMURA, M. KOBAYASHI, H.-M. KIM, F. MIYAJI and T. KOKUBO, *ibid.* **37** (1997) 265.
37. T. NAKAMURA, S. NISHIGUCHI, H.-M. KIM, F. MIYAJI and T. KOKUBO, in ''Advances in Science and Technology, vol. 28: Materials in Clinical Applications'' (Techna Srl, Faenza, 1999) p. 289.
38. S. NISHIGUCHI, T. NAKAMURA, M. KOBAYASHI, H.-M. KIM, F. MIYAJI and T. KOKUBO, *Biomaterials* **20** (1999) 491.
39. S. NISHIGUCHI, H. KATO, H. FUJITA, H.-M. KIM, F. MIYAJI, T. KOKUBO and T. NAKAMURA, *J. Biomed. Mater. Res.* **54** (1999) 689.
40. S. NISHIGUCHI, H. KATO, H. FUJITA, M. OKA, H.-M. KIM, T. KOKUBO and T. NAKAMURA, *Biomaterials* **22** (2001) 2522.
41. T. KOKUBO, H.-M. KIM, S. NISHIGUCHI and T. NAKAMURA, in ''Bioceramics'', vol. 13 (Trans Tech Pub., Switzerland, 2000) p. 3.
42. S. NISHIGUCHI, S. FUJIBAYASHI, H.-M. KIM, T. KOKUBO and T. NAKAMURA, *J. Biomed. Mater. Res.* **62A** (2003) 26.
43. H.-M. KIM, T. KOKUBO, S. FUJIBAYASHI, S. NISHIGUCHI and T. NAKAMURA, *J. Biomed. Mater. Res.* **52** (2000) 553.
44. S. NISHIGUCHI, H. KATO, M. NEO, M. OKA, H.-M. KIM, T. KOKUBO and T. NAKAMURA, *ibid.* **54** (2001) 198.
45. T. MIYAZAKI, H.-M. KIM, F. MIYAJI, T. KOKUBO and T. NAKAMURA, *ibid.* **50** (2000) 35.
46. T. MIYAZAKI, H.-M. KIM, F. MIYAJI, T. KOKUBO and T. NAKAMURA, *J. Mater. Sci.: Mater. Med.* **12** (2001) 683.
47. T. MIYAZAKI, H.-M. KIM, T. KOKUBO, C. OHTSUKI, H. KATO and T. NAKAMURA, *Biomaterials* **23** (2002) 827.
48. H. KATO, T. NAKAMURA, S. NISHIGUCHI, Y. MATSUSUE, M. KOBAYASHI, T. MIYAZAKI, H.-M. KIM and T. KOKUBO, *J. Biomed. Mater. Res.* **53** (2000) 28.

Received 14 August
and accepted 1 October 2003